JTTEE5 17:736–741
DOI: 10.1007/s11666-008-9256-3
1059-9630/$19.00 © ASM International

Peer Reviewed

Effect of Process Conditions on Microstructure and Corrosion Resistance of Cold-Sprayed Ti Coatings

Hong-Ren Wang, Bao-Rong Hou, Jun Wang, Qi Wang, and Wen-Ya Li

(Submitted May 13, 2008; in revised form September 21, 2008)

Ti and Ti alloys can be applied to steels as a protective coating in view of its excellent resistance to corrosive environment. Cold spraying, as a new coating technique, has potential advantages in fabrication of Ti coating in comparison with conventional thermal spraying techniques. In this study, Ti coatings were prepared on carbon steel substrates by cold spraying via controlling the process conditions. The microstructure of coatings was observed by SEM. The porosity of coatings was estimated by image analysis and the bond strength was tested for comparison of the process conditions. Potentiodynamic polarization and open-circuit potential (OCP) measurements were performed to understand the corrosion behavior of the coatings. The SEM examination shows that the coatings become more compact with the increases of pressure and temperature of driving gas. The potentiodynamic polarization curves indicate that the coating which has lower porosity has lower corrosion current. The polarization and OCP measurement reveal that cold-sprayed Ti coating can provide favorable protection to carbon steel substrate. The polishing treatment of coating surface polishes the rough outer layer including the small pores as well as decreases the actual surface area of the coating, leading to the considerable improvement of corrosion resistance.

Keywords cold spray, corrosion resistance, microstructure, process conditions, Ti coating

1. Introduction

Steels used in oceanic engineering are prone to corrosion and invalidation due to their lower corrosion resistance in marine environment. Titanium and its alloys have an excellent corrosion resistance in the severe marine environment and can be widely used for the protection of steel structures. So the corrosion resistance of steels can be improved by covering Ti coatings on their surfaces. Ti coatings are generally deposited by thermal spray process (Ref 1-6). However, owing to its high activity at elevated temperatures, thermal spraying of Ti in an air atmosphere usually results in a severely oxidized, unhomogeneous coating, which is brittle and porous. Therefore, in order to ensure the phase and chemical purity of Ti coatings, the spray process is usually conducted at a shrouded or low-pressure atmosphere, such as the shrouded plasma spray (APS/S), low-pressure plasma spray (LPPS). Other thermal spray technique is also used to produce dense Ti coatings such as modified HVOF spraying.

Cold spraying, as an emerging coating technique, has been developed to deposit high-quality metallic coatings. In this process, high pressure gas is introduced into a Laval type nozzle and produces a high-speed gas flow, and then spray particles are fed axially into the gas flow and accelerated to a high velocity (300-1200 m/s) and deposit through intensive plastic deformation upon impact on a substrate in a solid state and at a temperature well below the melting point of spray material (<600 °C) (Ref 7). According to lots of studies on cold spray since its invention, cold spraying is a suitable technique for production of most metals and their alloys (Ref 7-13), and even cermet coatings (Ref 14). It is generally accepted that there exists a critical velocity for a successful particle deposition. Only the particles have a velocity higher than this critical value can be deposited to form a coating. There are some reports concerned with the spray forming,

This article is an invited paper selected from presentations at the 2008 International Thermal Spray Conference and has been expanded from the original presentation. It is simultaneously published in *Thermal Spray Crossing Borders, Proceedings of the 2008 International Thermal Spray Conference*, Maastricht, The Netherlands, June 2-4, 2008, Basil R. Marple, Margaret M. Hyland, Yuk-Chiu Lau, Chang-Jiu Li, Rogerio S. Lima, and Ghislain Montavon, Ed., ASM International, Materials Park, OH, 2008.

Hong-Ren Wang and **Bao-Rong Hou**, Institute of Oceanology, Chinese Academy of Sciences, Qingdao 266071, People's Republic of China; **Hong-Ren Wang**, Graduate School of the Chinese Academy of Sciences, Beijing 100039, People's Republic of China; **Hong-Ren Wang, Jun Wang,** and **Qi Wang**, State Key Laboratory For Marine Corrosion and Protection, Luoyang Ship Material Research Institute (LSMRI), No.12A Jinhu Road, Qingdao 266071, Shandong Province, People's Republic of China; and **Wen-Ya Li**, Shaanxi Key Laboratory of Friction Welding Technologies, School of Materials Science and Engineering, Northwestern Polytechnical University, Xian 710072, People's Republic of China. Contact e-mail: wanghr@sunrui.net.

numerical simulation and experimental characterization, metal reactivity of cold spraying Ti coatings (Ref 15-19).

In the present study, the influence of process conditions, including gas type and its pressure and temperature on the microstructure and corrosion performance of cold-sprayed Ti coating were examined experimentally, compared with Ti bulk metal and carbon steel substrate, in order to optimize the process conditions and improve its anticorrosive property.

2. Materials and Experimental Procedures

2.1 Materials and Sample Preparation

Angular Ti powder sieved to the size from 5 to 45 μm was used as feedstock material, which was manufactured through hydrogenizing and dehydrogenating method. The composition of Ti powder is shown in Table 1. Carbon steel (Chinese trademark Q235A) plates were used as substrates. Prior to spraying, the substrate surface was sandblasted using 24 mesh alumina grits.

The cold spray system Cold Spray CS2000 was used to produce Ti coatings (Ref 13). The system included gas pressure regulators, gas preheater, powder feeder, and spray gun. The spray gun mainly consisted of a gas prechamber and a convergent-divergent accelerating nozzle. The nozzle had a throat diameter of 2 mm and an exit diameter of 6 mm. The length from the throat to the exit was 100 mm. The gas temperature and pressure in the prechamber were measured via the thermocouple and pressure gage mounted on the spray gun.

The driving gas used in cold spray process is pure N_2 or compressed air with a pressure up to 3 MPa, which is also used as the powder feeder gas synchronously. The controlled conditions of cold spray process applied to deposit different types of Ti coatings are listed in Table 2. In cold spraying process, the gun was controlled by a robot and the relative traverse speed of spray gun relative to substrate was 80 mm/s with a standoff distance of 15 mm.

2.2 Experimental Methods

The microstructure of Ti coating was characterized using an environmental scanning electron microscopy (ESEM, Philips XL-30) with voltage of 20 kV. The bond strength of coatings was tested using a WDW-20 tensile-testing machine at a rate of 10 mm/min with three parallel samples. The porosity of coatings was evaluated by image analysis with photoshop software.

The corrosion performance of Ti coatings was investigated in a 3.5wt.% NaCl solution at 30 °C using the as-sprayed and as-polished coatings, which were finished with Al_2O_3 abrasive paper from 220# to 1200# and polished with W2.5-μm silicon carbide abrasive on polishing cloth. The thickness of as-sprayed and as-polished Ti coatings was up to ~1 mm. The sample 2 Ti coatings were used for the open-circuit potential (OCP) measurement solely. The samples for polarization and OCP measurement were cut and sealed with epoxy to insulate the substrate and edges, only exposing a working coating surface of 10 × 10 mm. Samples of TA2 bulk metal and carbon steel substrate were prepared to the same dimension with a mechanical treatment surface. Samples for each polarization and OCP measurement had three parallel ones.

A Model 273A Potentiostat was used for potentiodynamic polarization measurement and a multicenter Potentiostat for OCP measurement. A saturated calomel electrode (SCE) with a Luggin capillary was used as a reference electrode, and a platinum wire twisted to a

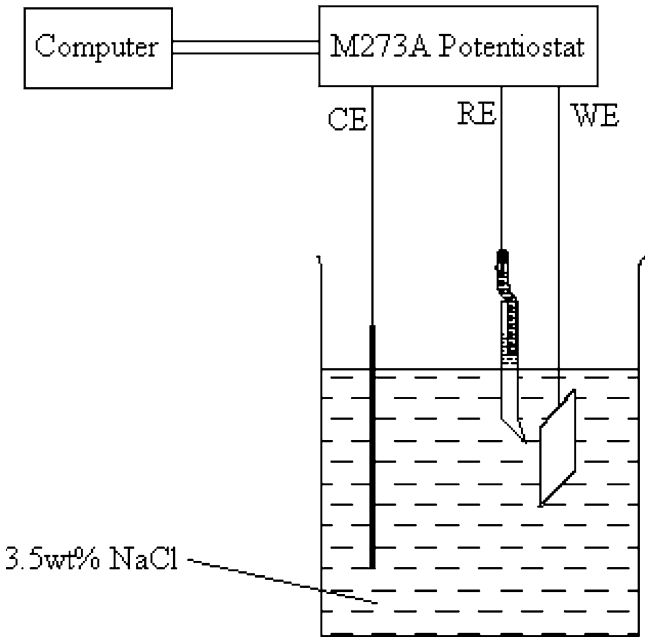

Fig. 1 Schematic diagram of electrochemical test system. CE, counter electrode; RE, reference electrode; WE, working electrode

Table 1 Composition of Ti powder

Element	O	Cl	H	N	C	Si	Fe	Ti
Composition, wt.%	0.33	0.03	0.024	0.056	0.01	<0.02	0.05	Bal.

Table 2 The controlled process conditions applied to deposit Ti coatings

Parameter	Sample 1	Sample 2	Sample 3	Sample 4	Sample 5	Sample 6
Driving gas	N_2	N_2	N_2	Compressed air	Compressed air	Compressed air
Temperature, °C	350 (T1)	500 (T2)	650 (T3)	500 (T2)	500 (T2)	500 (T2)
Pressure, MPa	2.0 (P1)	2.0 (P1)	2.0 (P1)	2.0 (P1)	1.8 (P2)	1.5 (P3)

multi-ring shape served as a counter electrode. Figure 1 shows the schematic diagram of the electrochemical test system. An initial delay time of 1 h was employed before polarization measurement. The polarization scan was started from 600 mV below the steady OCP to 600 mV over the OCP at a scanning rate of 10 mV/min. OCP measurement was carried out in 3.5wt.% NaCl solution for 30 days at an interval of 5-30 min according to the corrosion characteristic and experimental period.

3. Results and Discussion

3.1 Microstructure of Ti Coatings Using Different Operation Temperatures

Figure 2 shows the typical cross-sectional microstructure of cold-sprayed Ti coatings deposited using N_2 under a pressure of 2 MPa and temperatures of T1-T3. It is found that the interface of three kinds of coatings between the coating and substrate seems well bonded with little disfigurement. The average bond strength and porosity of coatings were listed in Table 3. It is found that the bond strength increases with the increase of gas temperature. And the density of coatings has also been enhanced obviously with increasing the gas temperature. The coating deposited under the temperature T3 has the most compact microstructure with porosity of 1.6%, and the coating under the temperature T1 has a relative porous structure with porosity of 10.3%.

It could be attributed to the increase of gas velocity due to the increase of gas temperature, which gives more kinetic energy to the particles. This enhances the plastic deformation during particle deposition. Further deformation of the previously deposited coating surface by the impacts of following particles is also obtained. The accumulative intensive deformation enhances the particle cohesion and leads to the formation of a dense coating (Ref 13).

3.2 Microstructure of Ti Coatings Using Different Operation Pressures

Figure 3 shows the typical cross-sectional microstructure of cold-sprayed Ti coatings deposited using compressed air under a temperature of T2 and pressures of P3 to P1. The bond strength and porosity were listed in Table 3. It can be found that the coating deposited under the pressure of P1 is denser with porosity of 10.0%. The coating becomes porous under the pressure of P2 with porosity of 14.8%, and the coating deposited under the pressure of P3 has the most porous microstructure with porosity of 17.5%. Table 3 shows that the coating bond strength increases with the increase of gas pressure.

It can be demonstrated that the density of coating could be improved by increasing the gas pressure. It could be attributed to the increase of gas velocity and dragging force due to the increase of gas pressure. The kinetic energy of particles is enhanced, leading to the formation of a denser coating (Ref 20).

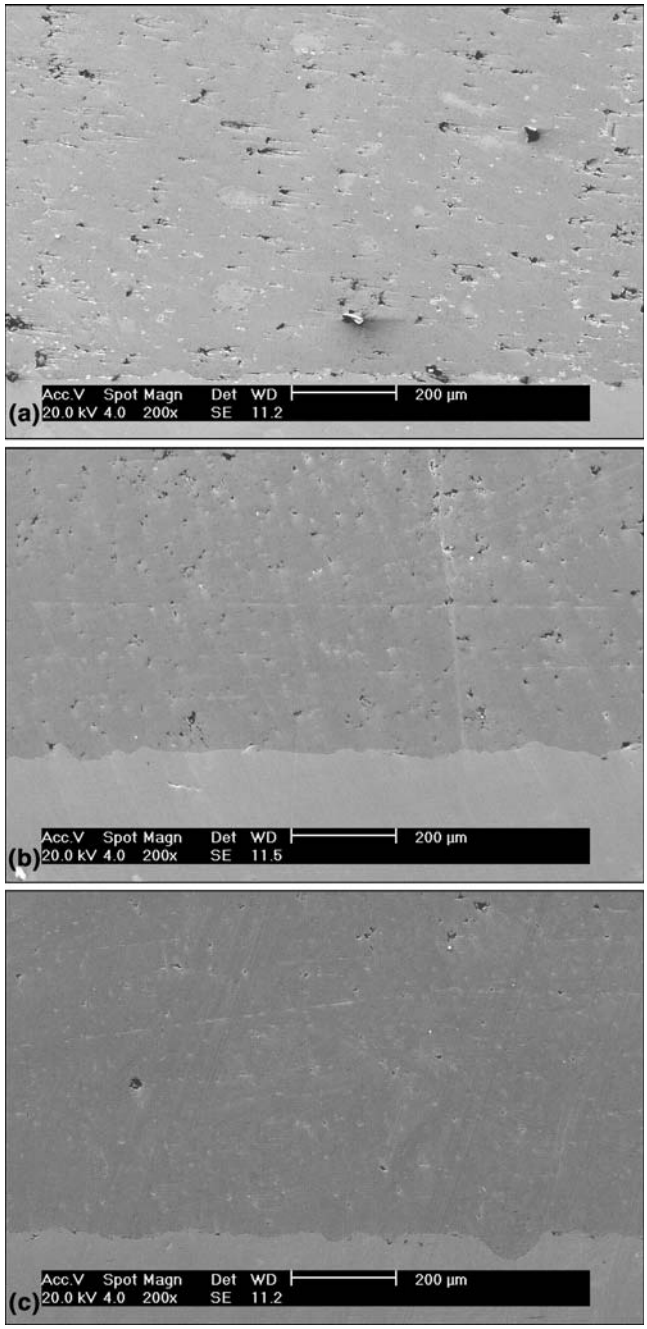

Fig. 2 Typical cross-sectional microstructure of cold-sprayed Ti coatings at the temperatures of (a) T1, (b) T2, and (c) T3 using N_2 under a pressure of P1

Table 3 Average bond strength and porosity of Ti coatings

Sample number	1	2	3	4	5	6
Bond strength, Mpa	9.4	11.2	16.1	10.3	10.0	8.7
Porosity, %	10.3	5.8	1.6	10.0	14.8	17.5

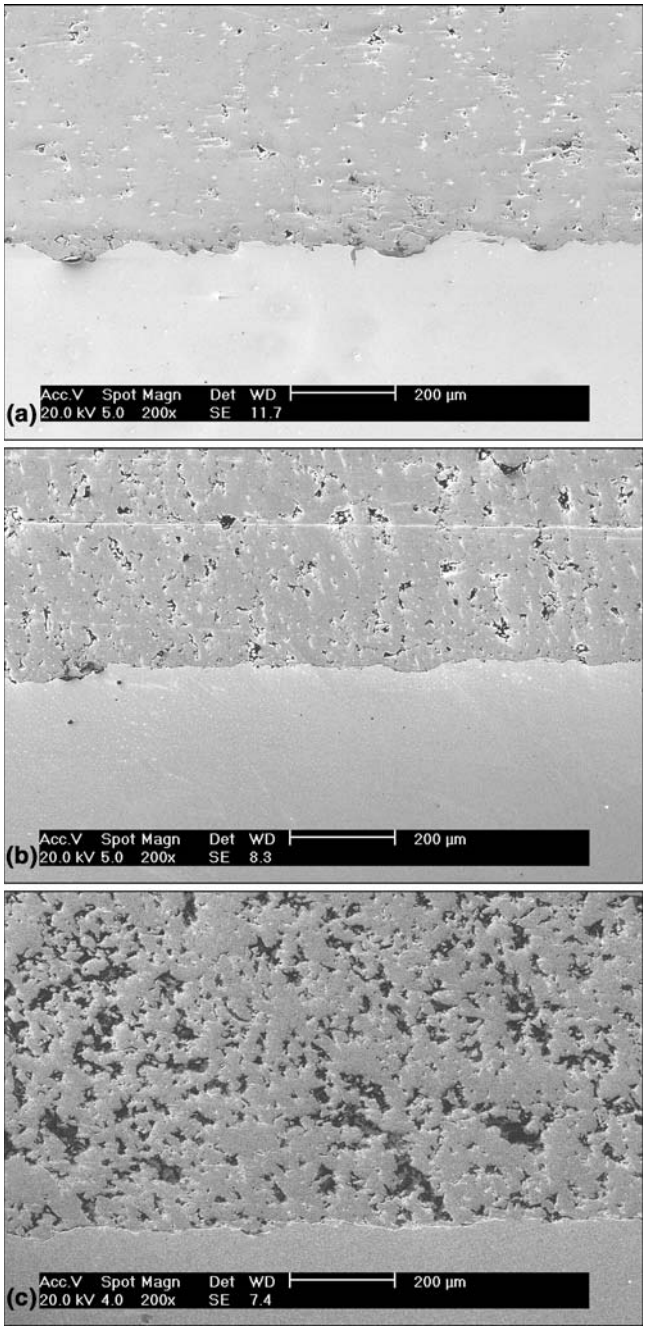

Fig. 3 Typical cross-sectional microstructure of cold-sprayed Ti coatings at the pressures of (a) P1, (b) P2, and (c) P3 using compressed air under a temperature of T2

3.3 Microstructure of Ti Coatings Using Different Driving Gas

Figure 2(b) and 3(a) show the comparison of the cross-sectional microstructure of different coatings using N_2 and compressed air as driving gas, respectively, under the same temperature and pressure. According Table 3, it is found that the coating deposited with N_2 has a much denser structure and higher bond strength than that deposited with air. The gas type has an evident influence on the

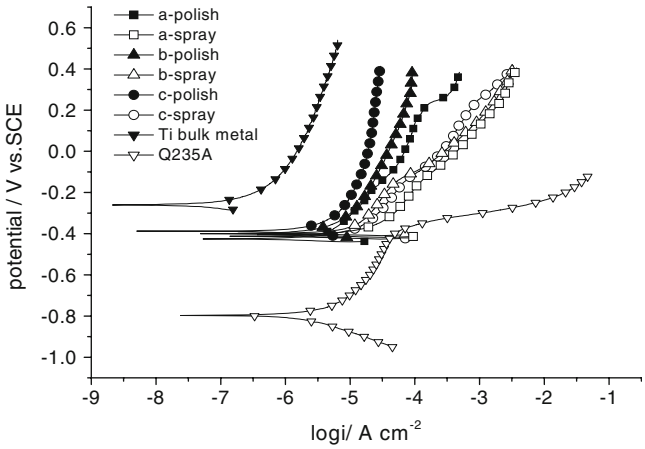

Fig. 4 Polarization curves of cold-sprayed Ti coatings at the pressures of (a) P3, (b) P2, and (c) P1 using compressed air under a temperature of T2 with TA2 bulk metal and Q235A substrate in 3.5wt.% NaCl

porosity of coating. The result is mainly attributed to the surface reactivity of Ti with oxygen. Besides particle velocity, the metal reactivity and oxide films at particle surfaces also take important roles on coating deposition process in cold spraying (Ref 17). The surface reactivity of Ti particle with oxygen in the adopted compressed air is evidently higher than that with entrained air by N_2 driving gas at the gun exit. This surface reaction could be helpful for the formation of a relative porous structure in compressed air (Ref 17-19).

3.4 Corrosion Resistance of Ti Coatings with Different Operation Conditions

Figure 4 shows the potentiodynamic polarization curves for the as-sprayed and as-polished Ti coatings using compressed air as driving gas under pressures of P3 to P1 at a temperature of T2. The as-polished coating has almost the similar polarization behavior with Ti bulk metal, but it has a larger polarization current due to their difference in density. The as-sprayed coatings have smaller polarization slope and larger polarization current compared with the as-polished coatings. It is clear that the polarization currents of coatings deposited under different pressures are different. The polarization current decreases with the increase of gas pressure, and the polarization current of as-sprayed surface is larger than the corresponding as-polished surface. This is because the polishing treatment peels the rough outer layer including small pores, as well as decreasing the actual surface area of the coating, leads to the considerable improvement of corrosion resistance.

As aforementioned, the coatings deposited under a lower pressure has more porous microstructure, the dissolved oxygen concentration is lower within the porous structure compared with the surrounding environment. Since Ti is a passive metal and its corrosion resistance depends on sufficient dissolved oxygen to keep its passivation in corrosive medium. The regions with lower dissolved oxygen concentration become the active corrosion

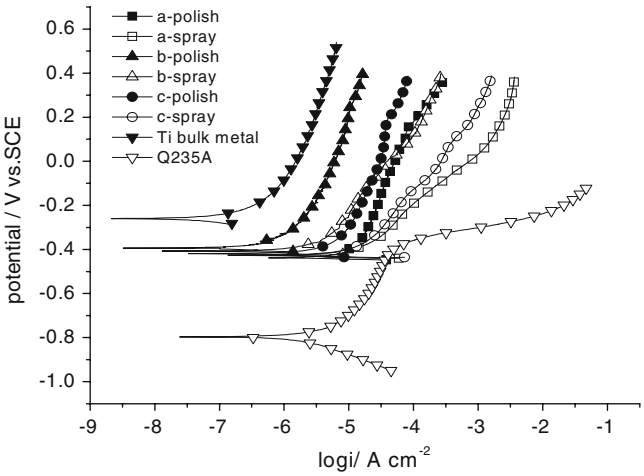

Fig. 5 Polarization curves of cold-sprayed Ti coatings at the temperatures of (a) T1, (b) T2, and (c) T3 using N_2 under a pressure of P1 with TA2 bulk metal and Q235A substrate 3.5wt.% NaCl

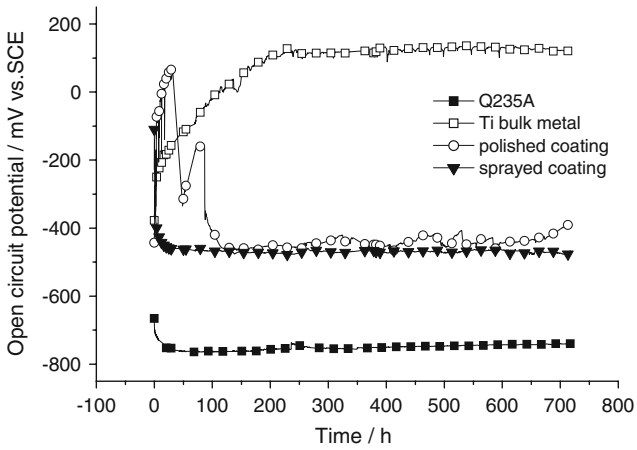

Fig. 6 Change of open-circuit potential versus immersion time of as-sprayed, as-polished sample-2 Ti coatings with TA2 bulk metal and Q235A substrate in 3.5wt.% NaCl

center and lead to the oxygen concentration difference corrosion (Ref 21).

Figure 5 shows the polarization curves of the as-sprayed and as-polished Ti coatings deposited using N_2 under different temperatures. There is obvious difference with polarization slope and current between the curves of coatings deposited under different temperatures. The as-polished coatings have higher corrosion resistance than the corresponding as-sprayed coatings.

According to Fig. 5, the coating deposited under the temperature T1 has the largest corrosion current density, and the coating deposited under the temperature T2 has the smallest one. The corrosion currents of coatings are correlative with the porosity and oxygen content on coating surface. The two factors influence the corrosion behavior of coating simultaneously and emulously. Due to the influence of the oxygen content to corrosion exceeds that of the density and keeps the dominant step, the corrosion current of coating deposited under T3 exceeds that of coating under T2.

According to the more negative corrosion potential and larger corrosion current of Q235A obtained from plorization curves in Fig. 4 and 5, the carbon steel substrate reveals much lower corrosion resistance than the coatings.

Figure 6 shows the change of OCP with immersion time for the as-sprayed and as-polished Ti coatings compared with TA2 bulk metal and Q235A substrate in 3.5wt.% NaCl. The OCP of TA2 bulk metal gradually shifts positively from −360 mV to 100 mV (SCE) in the initial stages of 200 h, subsequently achieves relatively steady OCP and finally keeps at 130 mV (SCE), indicating evident passivation occurs during immersion. The OCP of two coatings show negative shift due to initial corrosion. The OCP of as-sprayed coating achieves relatively steady state after 50 h and keeps at −470 mV (SCE), while the as-polished coating achieves steady OCP after 120 h and gradually shifts positively from −450 mV to −380 mV (SCE), indicating it is prone to achieve passivation than as-sprayed coating. The OCP of Q235A substrate keeps steadily at about −740 mV (SCE) due to its general corrosion.

The OCP of the coating was more negative than the TA2 bulk metal from 500 to 600 mV. It could be attributed to the porous surface structure of the coatings, which leads to a more active surface than that of TA2 (Ref 18). No evidence reveals that carbon steel substrate being corroded after 30 days immersion. It can be concluded from the OCP measurement that carbon steel substrate is favorable protected by coating.

4. Conclusions

For cold-sprayed Ti coatings, the gas pressure and temperature influence significantly the density of the deposited coatings. As the gas temperature increases, the porosity decreases. A higher gas pressure yields a lower porosity. The porosity of coating deposited using compressed air is relatively serious than coating deposited using N_2 under the same operation pressure and temperature due to the Ti reactivity with oxygen.

Potentiodynamic polarization results indicated that the coatings which had lower porosity had lower corrosion current. The polarization and OCP measurement reveals that cold-sprayed Ti coating has much higher corrosion resistance than carbon steel and can provide favorable protection to the substrate. The polishing treatment with coating surface peels the rough outer layer including the small pores, as well as decreasing the actual surface area of coating, leads to the considerable improvement of corrosion resistance.

Acknowledgment

This article is financially supported by the Foundation of China Shipbuilding Industry Corporation 03J2.2.1.

References

1. T. Kinos, S.L. Chen, P. Siitonen, and P. Kettunen, Corrosion Properties of Shrouded Plasma Sprayed Titanium Coatings, *Thermal Spraying—Current Status and Future Trends*, A. Ohmori, Ed. (Kobe, Japan), High Temperature Society of Japan, 1995, p 573-576
2. J. Kawakita, S. Kuroda, T. Fukushima, H. Katanoda, K. Matsuo, and H. Fukanuma, Dense Titanium Coatings by Modified HVOF Spraying, *Surf. Coat. Technol.*, 2006, **201**(3-4), p 1250-1255
3. E. Galvanetto, F.P. Galliano, F. Borgioli, U. Bardi, and A. Lavacchi, XRD and XPS Study on Reactive Plasma Sprayed Titanium-Titanium Nitride Coatings, *Thin Solid Films*, 2001, **384**(2), p 223-229
4. C.-E. Cui, Q. Miao, and J.-D. Pan, Ti/Cr Multi-Layer Coating on Magnesium Alloy AZ91 by Arc-Added Glow Plasma Depositing Technique, *Surf. Coat. Technol.*, 2007, **201**(9-11), p 5400-5403
5. J. Kawakita, H. Katanoda, M. Watanabe, K. Yokoyama, and S. Kuroda, Warm Spraying: An Improved Spray Process to Deposit Novel Coatings, *Surf. Coat. Technol.*, 2008, **202**(18), p 4369-4373
6. H.R. Salimijazi, T.W. Coyle, J. Mostaghimi, and L. Leblanc, Microstructure and Failure Mechanism in As-Deposited, Vacuum Plasma-Sprayed Ti-6Al-4V Alloy, *J. Therm. Spray Technol.*, 2005, **14**(2), p 215-223
7. A. Papyrin, A Cold Spray Technology, *Adv. Mater. Process*, 2001, **159**(9), p 49-51
8. T. Stoltenhoff, H. Kreye, and H.J. Richter, An Analysis of the Cold Spray Process and Its Coatings, *J. Therm. Spray Technol.*, 2002, **11**(4), p 542-550
9. R.C. McCune, W.T. Donlon, O.O. Popoola, and E.L. Cartwright, Characterization of Copper Layers Produced by Cold-Gas-Dynamic Spraying, *J. Therm. Spray Technol.*, 2000, **9**(1), p 73
10. T.H. Van Steenkiste, J.R. Smith, R.E. Teets, J.J. Moleski, D.W. Gorkiewicz, R.P. Tison, D.R. Marantz, K.A. Kowalsky, W.L. Riggs, P.H. Zajchowski, B. Pilsner, R.C. McCune, and K.J. Barnett, Kinetic Spray Coatings, *Surf. Coat. Technol.*, 1999, **111**(1), p 62
11. J. Karthikeyan, C.M. Kay, J. Lindeman, R.S. Lima, and C.C. Berndt, Cold Spray Processing of Titanium Powder, *Thermal Spray: Surface Engineering via Applied Research*, C.C. Berndt, Ed. (Materials Park, OH), ASM International, 2000, p 255-262
12. J. Karthikeyan, C.M. Kay, J. Lindemann, R.S. Lima, and C.C. Berndt, Cold Sprayed Nanostructured WC-Co, *Thermal Spray 2001: New Surfaces for a New Millennium*, C.C. Berndt, K.A. Khor, and E.F. Lugscheider, Eds., (Materials Park, OH), ASM International, 2001, p 383-387
13. C.-J. Li and W.-Y. Li, Deposition Characteristics of Titanium Coating in Cold Spray, *Surf. Coat. Technol.*, 2003, **167**(2-3), p 278-283
14. H.J. Kim, C.H. Lee, and S.Y. Hwang, Fabrication of WC-Co Coatings by Cold Spray Deposition, *Surf. Coat. Technol.*, 2005, **191**(2-3), p 335-340
15. T. Marrocco, D.G. McCartney, P.H. Shipway, and A.J. Sturgeon, Production of Titanium Deposits by Cold-Gas Dynamic Spray: Numerical Modeling and Experimental Characterization, *J. Therm. Spray Technol.*, 2006, **15**(2), p 263-272
16. R.E. Blose, Spray Forming Titanium Alloys Using the Cold Spray Process, *Thermal Spray Connects: Explore Its Surfacing Potential*, E. Lugscheider, Ed. (Düsseldorf, Germany), DVS, 2005 (in CD-ROM)
17. W.-Y. Li, C. Zhang, H.-T. Wang, X.-P. Guo, H.-L. Liao, C.-J. Li, and C. Coddet, Significant Influences of Metal Reactivity and Oxide Film of Powder Particles on Coating Deposition Characteristics in Cold Spraying, *Appl. Surf. Sci.*, 2007, **253**, p 3557-3562
18. H.R. Wang, W.Y. Li, J. Wang, Q. Wang, and L. Ma, Corrosion Behavior of Cold Sprayed Titanium Protective Coating on 1Cr13 Substrate in Seawater, *Surf. Coat. Technol.*, 2007, **201**(9-11), p 5203-5206
19. R.S. Lima, A. Kucuk, and C.C. Berndt, Deposition Efficiency, Mechanical Properties and Coating Roughness in Cold-Sprayed Titanium, *J. Mater. Sci. Lett.*, 2002, **21**, p 1687-1689
20. W.-Y. Li, C.-J. Li, Y.-Y. Wang, and G.-J. Yang, Effect of Parameters of Cold Sprayed Cu Particles on Its Impacting Behavior, *Acta Metall. Sin.*, 2005, **41**(3), p 282-286 (in Chinese)
21. J. Kawakita, T. Fukushima, S. Kuroda, and T. Kodama, Corrosion Behavior of HVOF Sprayed sus316L Stainless Steel in Sea Water, *Corros. Sci.*, 2002, **44**, p 2561-2581